Modeling Solid–Liquid Equilibrium of NH_4Cl-$MgCl_2$-H_2O System and Its Application to Recovery of NH_4Cl in MgO Production

Daoguang Wang and Zhibao Li

Key Laboratory of Green Process and Engineering, Institute of Process Engineering, National Engineering Laboratory for Hydrometallurgical Cleaner Production Technology, Chinese Academy of Sciences, Beijing 100190, P.R. China

DOI 10.1002/aic.12357

Published online August 3, 2010 in Wiley Online Library (wileyonlinelibrary.com).

A new method to recover NH_4Cl from NH_4Cl-rich aqueous solutions generated in the magnesia (MgO) production is developed on the basis of modeling the solid–liquid equilibrium (SLE) for the NH_4Cl-$MgCl_2$-H_2O system with the Pitzer model embedded in Aspen Plus™ platform. The SLE values for the ternary system were determined from 278.15 to 348.15 K. The new standard-state chemical potentials of NH_4Cl and $MgCl_2{\cdot}6H_2O$ were judicially obtained. The resulting equilibrium constants were used to determine new interaction parameters for the NH_4Cl-H_2O and $MgCl_2$-H_2O systems. These new parameters, together with the mixing parameters determined from correlating the experimental values, were used to correlate the equilibrium constant for $NH_4MgCl_3{\cdot}6H_2O$, which plays a key role in NH_4Cl recovery. The results could extend SLE calculation for the NH_4Cl-$MgCl_2$-H_2O system from 278.15 to 388.15 K, satisfying the process identification and simulation requirement involved in the recovery process. The phase-equilibrium diagram generated by modeling was illustrated to identify the process alternatives for recovering NH_4Cl. The resulting course to recover NH_4Cl by three fractional crystallization operations was finally proved feasible. © 2010 American Institute of Chemical Engineers *AIChE J,* 57: 1595–1606, 2011

Keywords: equilibrium, solubility, modeling, phase diagram, recovery, crystallization

Introduction

China is one of the countries rich in saline brine resources containing considerable amount of mainly magnesium and potassium. However, magnesium chloride is usually generated as byproduct or waste of the potassium fertilizer industry. The valuable magnesium resources cannot be used effectively and is discarded back into the sea or saline lakes, causing a serious environmental problem. Therefore, extraction and application of magnesium resources existing in saline brine is growing interesting from an ecological, economic, and technological point of view.

Correspondence concerning this article should be addressed to Z. Li at zhibaoli@mail.ipe.ac.cn.

An attractive way to beneficiate magnesium chloride brine is to prepare high-quality MgO. Considerable efforts have been done to develop the methods to produce MgO from sea-lake brine of high magnesium content. Aman process,[1] in which MgO is prepared from direct decomposition of bischofite by reaction (1), is industrially used but has the disadvantage of high equipment cost and energy cost for releasing HCl (very corrosive) and repeating calcinations.

$$MgCl_2 \cdot 6H_2O \rightarrow MgO + 2HCl + 5H_2O \qquad (1)$$

An alternative way is the conversion of magnesium to $Mg(OH)_2$, from which MgO was subsequently obtained by calcination, by the reaction with lime or ammonia.[1] This method badly encounters difficulty in the solid–liquid

separation of $Mg(OH)_2$ suspension for its small particle size and gelatinous state. A novel process currently under development was proposed by authors[2,3] to extract magnesium by reaction (2) for precipitation of magnesium carbonate compounds, i.e., nesquehonite or hydromagnesite because of their good filtration properties.

$$MgCl_2 + (NH_4)_2CO_3 + H_2O \rightarrow \text{Magnesium carbonate compounds} + NH_4Cl \quad (2)$$

Following the reaction, magnesium carbonate compounds are separated by filtration to obtain high-quality magnesia (MgO) upon drying and calcination, leaving behind an ammonium chloride–water mixture. The tough problem is how to regenerate or recover the valuable byproducts.

There are two approaches currently applied in industrial soda process for ammonium regeneration. One is called Solvay soda process in which the ammonia is regenerated for recycle by use of lime. However, the usage of lime renders the process ineffective mainly because the calcination of limestone to lime yields the emission of CO_2 and extensive energy consumption.[4] Furthermore, a huge amount of calcium chloride containing waste is discarded to environment. The other, an alternative approach, is called combination soda process (Hou's).[5] Ammonium chloride is recovered as saleable product by crystallization process with the aid of common-ion effect of NaCl to NH_4Cl-rich solutions.

Referring to Hou's soda process, a new method to recover crystalline NH_4Cl as saleable product in the process of MgO production is proposed by feeding magnesium chloride, instead of sodium chloride, into the NH_4Cl-rich solutions generated. The advantage of $MgCl_2$ over NaCl in the recovery of NH_4Cl is its stronger common-ion effect because $MgCl_2$ yields two chloride ions instead of one from NaCl in an aqueous solution. It is known that the solubility and phase equilibrium of salts in electrolyte aqueous solutions play a significant role in the development, design, optimization, and operation of crystallization processes.[6–8] The determination and estimation of solubility of the NH_4Cl-$MgCl_2$-H_2O system can prove invaluable in controlling the supersaturation in NH_4Cl crystallization process with the help of addition of $MgCl_2$. The solubility data of the NH_4Cl-$MgCl_2$-H_2O system are available in some literatures,[9] and the thermodynamic models for the ternary system at 298.15 K have also been established by Balarew and Guedouzi.[10–12] However, most of the previous studies have been focused on the solubility of the ternary system at ambient temperature and are not sufficient to the development of NH_4Cl recovery process. To substantiate the database for establishing a correlation of the temperature effect on solubility, and find the optimal course of crystallization to recover NH_4Cl from NH_4Cl-rich solutions generated in the process of MgO production, a further study on the NH_4Cl-$MgCl_2$-H_2O ternary system is necessary.

The objective of this article is to establish an accurate, comprehensive, self-consistent model which is capable of predicting the solubility of the NH_4Cl-$MgCl_2$-H_2O ternary system in the entire concentration and temperature range and to develop the course of crystallization for recovering NH_4Cl in the process of MgO production. To be concrete, the solid–liquid equilibrium (SLE) values for the ternary system are determined by isothermal dissolution method.[13,14] The Pitzer activity coefficient model embedded in the commercial Aspen Plus™ software is adopted for data correlation to satisfy process development and simulation. New Pitzer interaction parameters of pure NH_4Cl and $MgCl_2{\cdot}6H_2O$ are correlated using equilibrium constants resulting from judicially obtained standard-state chemical potentials for NH_4Cl and $MgCl_2{\cdot}6H_2O$, whereas the Pitzer mixing parameters are correlated using the experimental data together with some of the literature values. The parameters obtained are used to regress the equilibrium constant of $NH_4MgCl_3{\cdot}6H_2O$. Then, the visualization of phase behavior is constructed through systematic experimental determination of any missing solubility data and the thermodynamic regression of all the available data, and how the resulting phase diagram can aid the process synthesis activities is demonstrated. Finally, the proposed method is experimentally proved.

Experimental

Chemical agents

Ammonium chloride (99.5%, Beijing Chemical Plant) and magnesium chloride hexahydrate (98%, Beijing Chemical Plant) used in the experiments were of analytical grade without further purification. A series of magnesium chloride solutions, concentrations range from 0.5 mol L^{-1} to saturation with an interval of 0.5 mol L^{-1}, were prepared by dissolving magnesium chloride hexahydrate in double distilled water (conductivity < 0.1 μS cm^{-1}).

Procedure for solid–liquid equilibrium determination

A typical experimental procedure is performed as follows. The 150 mL of $MgCl_2$ solution was introduced to glass reactor (effective volume 250 mL), which was equipped with a magnetic stirrer and capped with glass stoppers. The reactors were then immersed in a temperature-controlled water bath, allowing the solution to stir continuously for about 0.5 h to establish the temperature equilibrium. The temperature was kept constant within 0.1 K. Then, slightly excess solid of NH_4Cl was added bit by bit to the $MgCl_2$ solutions in reactors. The standard equilibration time used was 6 h. After the SLE was attained, stirring was stopped to allow solids to settle by 6 h. The clear supernatant solution was then withdrawn and immediately injected into a 25-mL volumetric flask, which was kept in the water bath, being heated to bath temperature for measuring the density of saturated solution.

The composition of the saturated solutions was analyzed by volumetric methods, the error ranging from 0.1 to 0.2%. The Mg^{2+} concentration was determined by complexometric titration with EDTA at pH 9.5–10 (ammonia buffer), using Eriochrome black T as the indicator. The NH_4^+ ion concentration was determined by formaldehyde method with titration of NaOH, using methyl red and phenolphthalein as the indicators. The solid phase was filtered and washed with water. The washed solid was dried at 323.15 K for 12 h and analyzed by X-ray powder diffraction (XRD) to determine the final solid phase. Additionally, the double salts obtained were also identified thermodynamically with TGA (Q5000) apparatus as samples of $\sim$10 mg which were placed in a

corundum crucible and heated to 1073.15 K under N_2 with a heating rate of 10 K min^{-1}.

Procedure for the recovery of NH_4Cl

The experiments for the recovery of NH_4Cl from NH_4Cl-rich solution were performed in a 1-L jacketed glass reactor connected with a water circulator. The experiment consists of three steps, which were described as later section in this work. The crystals obtained in the experiments were dried at 323.15 K for 12 h and subjected to XRD and scanning electron microscopy (SEM) analysis to validate the developed method for the recovery of NH_4Cl.

Thermodynamic Modeling Framework

Chemical equilibrium relationships

Three possible solubility equilibria existing in NH_4Cl-$MgCl_2$-H_2O system can be described by the following dissolution reactions:

$$NH_4Cl(s) = NH_4^+ + Cl^- \tag{3}$$

$$MgCl_2 \cdot 6H_2O(s) = Mg^{2+} + 2Cl^- + 6H_2O \tag{4}$$

$$NH_4MgCl_3 \cdot 6H_2O(s) = NH_4^+ + Mg^{2+} + 3Cl^- + 6H_2O. \tag{5}$$

Their equilibrium constants (also called solubility product) are designated as K_1 for NH_4Cl, K_2 for $MgCl_2{\cdot}6H_2O$, and K_3 for the double salt, $NH_4MgCl_3{\cdot}6H_2O$. The equilibrium constants should be known in advance before any SLE calculation. In this work, the basis of calculations will be molality-based equilibrium constants for the various salts of interest, which is defined as follows:

$$K_{j,T} = \prod a_i^{v_i} = \prod \gamma_{\pm}^{\sum v_i} m_i^{v_i} \cdot a_{H_2O}^{v_{H_2O}}, \tag{6}$$

where

$$\gamma_{\pm} = \left(\prod \gamma_i^{v_i}\right)^{1/\sum v_i}. \tag{7}$$

The equilibrium constant can be calculated by Van't Hoff equation:

$$\ln K_T = -\frac{\Delta\mu_r^0}{RT_r} - \frac{\Delta H_r^0}{R}\left(\frac{1}{T} - \frac{1}{T_r}\right) - \int_{T_r}^{T} \frac{1}{RT^2} \int_{T_r}^{T} \Delta C_p dT dT, \tag{8}$$

where $\Delta\mu_r^0$ and ΔH_r^0 are molar reaction chemical potential and molar reaction enthalpy, respectively, and their values are calculated by a judicial method,[15] which will be discussed in the later section. Unfortunately, the enthalpy, the entropy, and the heat capacity are not available for $NH_4MgCl_3{\cdot}6H_2O$, thus K_3 is regressed with newly obtained model parameters.

The Pitzer activity coefficient model and water activity relationships

There are different types of activity coefficient models that may be used in this context. Pitzer model has been successfully used for highly concentrated electrolytes (up to 30 m) and elevated temperature (up to 473 K). Hence, it is appropriate for the present system, which is up to 20 m and 388 K. Pitzer[16,17] described the equation for activity coefficient of a 1-1 electrolyte NX in a common-ion mixture with a 2-1 electrolyte MX by:

$$\begin{aligned}\ln \gamma_{NX} =& f^{\gamma} + \frac{1}{3}(2+y)I\left[B_{NX} + \frac{1}{3}(2+y)IC_{NX}\right] \\ &+ yI\left[B_{NX} + \frac{1}{3}(2+y)IC_{NX}\right] \\ &+ \frac{1}{3}(1-y)I\left[B_{MX} + \frac{1}{3}(2+y)IC_{MX} + \theta_{MN}\right] \\ &+ \frac{1}{3}y(2+y)I^2(B'_{NX} + C_{NX}) \\ &+ \frac{(1-y)(2+y)}{9}I^2\left(B'_{MX} + C_{MX} + \frac{1}{2}\psi_{MNX}\right) \\ &+ \frac{(1-y)y}{6}I^2\psi_{MNX}\end{aligned} \tag{9}$$

and

$$\begin{aligned}\ln \gamma_{MX} =& 2f^{\gamma} + \frac{2}{9}(2+y)I\left[B_{MX} + \frac{1}{3}(2+y)IC_{MX}\right] \\ &+ \frac{4}{9}(1-y)I\left[B_{MX} + \frac{1}{3}(2+y)IC_{MX}\right] \\ &+ \frac{4}{3}yI\left[B_{NX} + \frac{1}{3}(2+y)IC_{NX} + \frac{1}{2}\theta_{MN}\right] \\ &+ \frac{2}{9}(1-y)(2+y)I^2\left(B'_{MX} + \frac{2}{3}C_{MX}\right) \\ &+ \frac{2y(2+y)}{3}I^2\left(B'_{NX} + \frac{2}{3}C_{NX} + \frac{1}{2}\psi_{MNX}\right) \\ &+ \frac{2(1-y)y}{9}I^2\psi_{MNX},\end{aligned} \tag{10}$$

where

$$f^{\gamma} = -A_{\varphi}\left[\frac{I^{1/2}}{1+bI^{1/2}} + \frac{2}{b}\ln(1+bI^{1/2})\right] \tag{11}$$

$$B_{MX} = \beta_{MX}^{(0)} + \frac{2\beta_{MX}^{(1)}}{\alpha^2 I}\left[1 - (1+\alpha I^{1/2})\exp(-\alpha I^{1/2})\right] \tag{12}$$

$$B'_{MX} = \frac{2\beta_{MX}^{(1)}}{\alpha^2 I^2}\left[-1 + \left(1 + \alpha I^{1/2} + \frac{1}{2}\alpha^2 I\right)\exp(-\alpha I^{1/2})\right] \tag{13}$$

$$C_{MX} = \frac{C_{MX}^{\phi}}{2|z_M z_X|^{1/2}} \tag{14}$$

For the system considered in this work, the values of the empirical parameters b and α were taken to be 1.2 and 2.0 $(kg/mol)^{-1/2}$, respectively.[17] A_{φ} is the Debye-Hückel parameter for the osmotic coefficient, which was obtained from the work of Pitzer.[17]

Finally, the solvent activity, a_{H_2O}, is related to the osmotic coefficient, ϕ, according to

$$\ln a_{H_2O} = -\frac{\phi \sum m_i}{55.5087}. \tag{15}$$

Table 1. Experimental Solubilities in the NH_4Cl-$MgCl_2$-H_2O System

$m(MgCl_2)$ / mol · kg^{-1}	$m(NH_4Cl)$ / mol · kg^{-1}	ρ / g · mL^{-1}	Solid	$m(MgCl_2)$ / mol · kg^{-1}	$m(NH_4Cl)$ / mol · kg^{-1}	ρ / g · mL^{-1}	Solid
T = 278.15 K				T = 283.15 K			
0.5257	4.8924	1.0921	N	0.5190	5.2357	1.0927	N
1.4724	3.5499	1.1309	N	1.4667	3.7010	1.1327	N
2.5975	2.0624	1.1839	N	2.5779	2.2813	1.1834	N
3.2213	1.5585	1.2127	N + NM	3.2534	1.7485	1.2117	N + NM
3.5550	0.7448	1.2284	NM	3.3445	1.3349	1.2182	NM
3.9770	0.3428	1.2444	NM	3.9917	0.4090	1.2435	NM
4.5700	0.0771	1.2759	NM	4.5728	0.0936	1.2747	NM
5.5561	0.0100	1.3324	NM + M	5.6400	0.0116	1.3333	NM + M
T = 288.15 K				T = 293.15 K			
0.5186	5.5365	1.0942	N	0.5193	5.8925	1.0954	N
1.4433	3.9975	1.1320	N	1.4477	4.3196	1.1328	N
2.5933	2.5312	1.1827	N	2.5989	2.9006	1.1819	N
3.2692	1.9553	1.2125	N + NM	3.2739	2.1489	1.2122	N + NM
3.4655	1.2724	1.2226	NM	3.5974	1.1865	1.2263	NM
4.0026	0.5005	1.2426	NM	4.0259	0.6037	1.2411	NM
4.5828	0.1166	1.2735	NM	4.5677	0.1464	1.2727	NM
5.6366	0.0136	1.3339	NM + M	5.7410	0.0157	1.3334	NM + M
T = 298.15 K				T = 303.15 K			
0.0000	7.3203	1.0874	N	0.0000	7.6065	1.0781	N
0.5149	6.4629	1.0941	N	0.5116	6.6736	1.0974	N
1.0542	5.5175	1.1260	N	1.0520	5.6319	1.1162	N
1.5931	4.5576	1.1489	N	1.5915	4.7160	1.1393	N
2.1332	3.6788	1.1624	N	2.1406	3.9148	1.1624	N
2.7250	2.9532	1.1893	N	2.7272	3.1474	1.1881	N
3.2555	2.3978	1.2103	N + NM	3.2721	2.6005	1.2111	N + NM
3.2358	2.4129	1.2125	N + NM	3.3609	2.2580	1.2142	NM
3.8320	0.8867	1.2363	NM	3.7929	1.1195	1.2320	NM
4.4081	0.2107	1.2676	NM	4.4931	0.2730	1.2635	NM
5.1443	0.0570	1.3049	NM	5.2040	0.0844	1.2947	NM
5.6241	0.0235	1.3332	NM	5.7888	0.0231	1.3277	NM
5.7797	0.0166	1.3357	NM + M	5.8917	0.0195	1.3358	NM + M
5.7554	0.0000	1.3353	M	5.8795	0.0000	1.3358	M
T = 308.15 K				T = 313.15 K			
0.0000	8.0160	1.0786	N	0.0000	8.3879	1.0794	N
0.5182	7.0672	1.0909	N	0.5099	7.3776	1.0980	N
1.0600	6.0284	1.1176	N	1.0485	6.3453	1.1170	N
1.6040	5.0736	1.1392	N	1.5901	5.3902	1.1399	N
2.1600	4.2396	1.1624	N	2.1249	4.5389	1.1621	N
2.7398	3.4392	1.1868	N	2.7293	3.7190	1.1860	N
3.3307	2.8429	1.2090	N + NM	3.3171	3.0695	1.2109	N + NM
3.3439	2.6455	1.2126	NM	3.3578	3.0605	1.2134	N + NM
3.7913	1.2829	1.2301	NM	3.6540	1.4319	1.2308	NM
4.4936	0.3478	1.2626	NM	4.4350	0.4235	1.2610	NM
5.1776	0.0987	1.2936	NM	5.1555	0.1252	1.2920	NM
5.6836	0.0310	1.3278	NM	5.9341	0.0364	1.3261	NM
5.8410	0.0209	1.3368	NM + M	6.0473	0.0250	1.3381	NM + M
5.8488	0.0000	1.3371	M	6.0583	0.0000	1.3370	M
T = 318.15 K				T = 323.15 K			
0.0000	8.7694	1.0794	N	0.0000	9.3852	1.0810	N
0.5146	7.7730	1.0987	N	0.5145	8.3234	1.0990	N
1.0605	6.7675	1.1183	N	1.0620	7.2776	1.1182	N
1.6107	5.7927	1.1398	N	1.6172	5.9476	1.1386	N
2.1413	4.8651	1.1620	N	2.1370	5.2198	1.1713	N
2.7324	4.0120	1.1840	N	2.7411	4.4201	1.1846	N
3.4048	3.3015	1.2084	N + NM	3.3520	3.6073	1.2129	N + NM
3.5648	2.3110	1.2323	NM	3.7244	2.3295	1.2215	NM
3.8672	1.4309	1.2321	NM	3.9349	1.6396	1.2319	NM
4.4821	0.5108	1.2600	NM	4.5675	0.5583	1.2616	NM
5.1747	0.1508	1.2930	NM	5.2395	0.1775	1.2912	NM
6.0724	0.0349	1.3245	NM	5.8974	0.0642	1.3233	NM
6.1085	0.0343	1.3399	NM + M	6.1836	0.0330	1.3425	NM + M
6.1297	0.0000	1.3406	M	6.2424	0.0000	1.3431	M

(*Continued*)

Table 1. (Continued)

$m(MgCl_2)$ / mol · kg^{-1}	$m(NH_4Cl)$ / mol · kg^{-1}	ρ / g · mL^{-1}	Solid	$m(MgCl_2)$ / mol · kg^{-1}	$m(NH_4Cl)$ / mol · kg^{-1}	ρ / g · mL^{-1}	Solid
$T = 328.15$ K				$T = 333.15$ K			
0.0000	9.7593	1.0809	N	0.0000	10.2421	1.0794	N
0.5169	8.6841	1.0993	N	0.5051	9.1088	1.0994	N
1.0586	7.6415	1.1194	N	1.0361	8.1025	1.1175	N
1.6089	6.6219	1.1394	N	1.5464	6.9202	1.1486	N
2.1617	5.7158	1.1609	N	2.1354	6.0632	1.1575	N
2.7335	4.6625	1.1826	N	2.7091	5.1221	1.1792	N
3.4450	3.8336	1.2125	N + NM	3.3427	4.3531	1.2076	N + NM
3.6670	2.7074	1.2207	NM	3.4128	4.1505	1.2097	NM
3.8918	1.8746	1.2311	NM	3.8101	2.5086	1.2267	NM
4.5217	0.6848	1.2586	NM	4.4967	0.8525	1.2553	NM
5.1943	0.2153	1.2894	NM	5.2054	0.2576	1.2883	NM
5.9374	0.0711	1.3214	NM	5.8558	0.0989	1.3175	NM
6.2867	0.0357	1.3445	NM + M	6.3425	0.0612	1.3360	NM + M
6.3544	0.0000	1.3455	M	6.4113	0.0000	1.3455	M
$T = 338.15$ K				$T = 343.15$ K			
0.0000	10.6690	1.0801	N	0.0000	11.1809	1.0827	N
0.5009	9.3952	1.0994	N	0.5033	9.9897	1.0996	N
1.0350	8.4488	1.1165	N	1.0476	8.8924	1.1170	N
1.5695	7.4133	1.1375	N	1.5576	7.7910	1.1370	N
2.1230	6.4187	1.1593	N	2.1282	6.8093	1.1579	N
2.7097	5.4639	1.1816	N	2.7121	5.8742	1.1791	N
3.3301	4.6334	1.2226	N + NM	3.3358	4.9273	1.2028	N + NM
3.5046	4.3265	1.2114	NM	3.5287	4.5483	1.2110	NM
3.7726	2.9682	1.2225	NM	3.8048	3.2878	1.2223	NM
4.3906	1.0599	1.2514	NM	4.3696	1.4999	1.2449	NM
5.2967	0.3212	1.2860	NM	5.2208	0.4187	1.2829	NM
5.8688	0.1365	1.3151	NM	5.9545	0.1472	1.3122	NM
6.4062	0.0769	1.3335	NM + M	6.2997	0.1045	1.3300	NM + M
6.5482	0.0000	1.3508	M	6.7483	0.0000	1.3496	M
$T = 348.15$ K							
0.0000	11.5053	1.0836	N				
0.5037	10.4235	1.0965	N				
1.0289	9.2682	1.1166	N				
1.5802	8.2490	1.1362	N				
2.1320	7.2109	1.1579	N				
2.7027	6.2107	1.1778	N				
3.3798	5.3854	1.2024	N + NM				
3.6486	5.0006	1.2140	NM				
3.8973	3.6040	1.2230	NM				
4.2281	2.3089	1.2370	NM				
5.1215	0.5976	1.2754	NM				
5.8491	0.2096	1.3036	NM				
6.3463	0.1319	1.3260	NM + M				
6.8209	0.0000	1.3531	M				

Solid: N-NH_4Cl(s), M-$MgCl_2{\cdot}6H_2O$(s), NM-$NH_4MgCl_3{\cdot}6H_2O$(s).

Results and Discussion

Experimental solubility

The experimental solubility determined at various temperatures of total concentration range is listed in Table 1, reported on the solvent-free basis. A comparison of solubility of NH_4Cl in the NH_4Cl-$MgCl_2$-H_2O system reported in the literature at 298.15 K with our experimental results is depicted in Figure 1, indicating that the experimental results are consistent with the literature values.[9] The analysis of equilibrated salts shows that the ternary NH_4Cl-$MgCl_2$-H_2O system exhibits a double salt, ammonium carnallite, having a formula, $NH_4MgCl_3{\cdot}6H_2O$. Thus, as can be observed in Figure 1, a typical solubility curve for NH_4Cl-$MgCl_2$-H_2O system consists of three branches: NH_4Cl and $NH_4MgCl_3{\cdot}6H_2O$ with broad fields of crystallization as well as $MgCl_2{\cdot}6H_2O$ with a very narrow field of crystallization.

Solubility representation using the Pitzer model

Previous studies[10–12] demonstrated that the Pitzer ion-interaction model has been successfully applied for thermodynamic analysis of experimental solubility data of the NH_4Cl-$MgCl_2$-H_2O system at 298.15 K. However, the Pitzer model parameters that they obtained were not demonstrated to be applicable to calculate the SLE for the ternary NH_4Cl-$MgCl_2$-H_2O system at elevated temperatures. Hence, these models cannot be used to simulate the practical NH_4Cl crystallization process with the addition of $MgCl_2$ because this

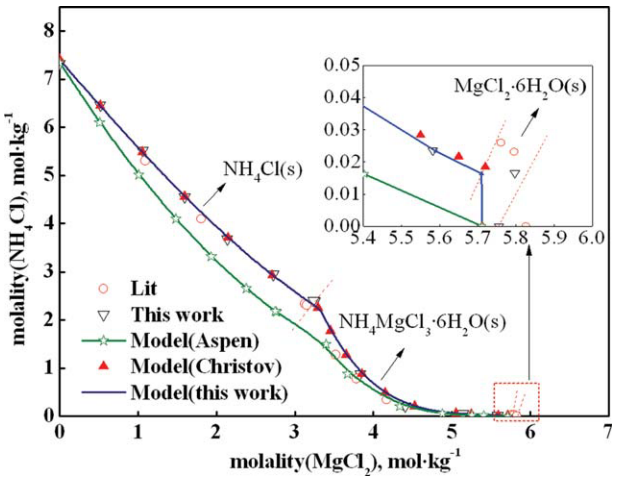

Figure 1. Solubility in the ternary NH_4Cl-$MgCl_2$-H_2O system at 298.15 K.

[Color figure can be viewed in the online issue, which is available at wileyonlinelibrary.com.]

process operates in a wide temperature range from 273.15 to 373.15 K. Another thermodynamic model based on Pitzer approach that potentially can be used for the calculation of the SLE for the ternary NH_4Cl-$MgCl_2$-H_2O system is the one that forms the basis of Aspen Plus™ platform. Preliminary predictions of solubility data of NH_4Cl-$MgCl_2$-H_2O system and comparison with experimental data generated by the authors and literature data yielded poor results, not to mention Aspen's inability to address ammonium carnallite $NH_4MgCl_3{\cdot}6H_2O$. Given, however, the attractiveness of regression ability incorporated in Aspen Plus™ platform and the user friendly interface of it, further work was undertaken with the purpose of improving Aspen's SLE estimation capability via determination and validation of new Pitzer model parameters.

Calculation of Equilibrium Constants K_1 and K_2. There are mainly three methods for acquiring the equilibrium constants.[15] In method 1, the equilibrium constants can be determined from the solubility of a single electrolyte in pure water using an adequate model for describing the activity coefficients, method 2 from the chemical potentials of the equilibrium species by Van't Hoff equation as Eq. 8, and method 3 from the experimental data and the activity coefficients of the components of the solutions. Method 2 is generally the first choice because the accuracy of K values is independent of the solubility data as well as the model used to describe the activity coefficients.[18–21] Therefore, in this work, the values of K_1 and K_2 were determined by method 2. However, K values are quite sensitive to the chemical potentials of the equilibrium species. Preliminary solubility calculation with the standard-state chemical potentials of equilibrium species including NH_4Cl and $MgCl_2{\cdot}6H_2O$ salts reported by literatures[22] gave poor results. Thus, in this work, the standard-state chemical potentials of NH_4Cl and $MgCl_2{\cdot}6H_2O$ salts were estimated by means of Eq. 16 with equilibrium constants (K_{j,T_r}) having the values of 2.86[10] and 10.397[23] for NH_4Cl and $MgCl_2{\cdot}6H_2O$, respectively, as shown in Table 2.[10,23–31]

Table 3. Standard-State Chemical Potentials, Enthalpies of Formation, and Entropies of Species

Species	$-\mu^0$ kJ · mol^{-1}	$-\Delta_f H^0$ kJ · mol^{-1}	S^0 J · mol^{-1} · K^{-1}
$Cl_2(g)$[22]			223.00
$H_2(g)$[22]			130.68
$N_2(g)$[22]			191.61
$O_2(g)$[22]			205.03
$Mg(s)$[22]			32.60
$Cl^-(aq)$[32,33]	131.290	167.080	56.735
$NH_4^+(aq)$[32,33]	79.451	133.260	111.169
$Mg^{2+}(aq)$[32,33]	454.289	466.271	−138.164
$H_2O(l)$[34]	237.178	285.830	69.94
$NH_4Cl(s)$[22]	*203.650**	*315.100**	94.86
$MgCl_2{\cdot}6H_2O(s)$[22]	*2114.163**	*2498.307**	366.345

*This work.

$$\mu_j^0 = \sum \nu_{ji}\mu_{ji}^0 + RT_r \ln K_{j,T_r}. \tag{16}$$

Other relevant thermodynamic data at standard state for ions, i.e., NH_4^+, Mg^{2+}, and Cl^-, together with the temperature functions of their heat capacities, were taken from Shock, Helgeson, and Sverjensky[32,33] and are listed in Tables 3 and 4, respectively. The entropies of ammonium chloride and magnesium chloride haxehydrate at 298.15 K were compiled by Barrow,[22] and heat capacities were taken from Pubic databank embedded in the OLI systems.[34] The values of $\Delta_f H_j^0$ were then obtained by

$$\Delta_f H_j^0 = \mu_j^0 + T_r(S_{j,T_r}^0 - \sum_n \frac{\kappa_{j,n} S_{n,T_r}^0}{2}), \tag{17}$$

where n presents the simple substance, i.e., H_2, N_2, O_2, Cl_2, and Mg, with respect to the element involved in salts. All of the calculated results of μ^0 and $\Delta_f H^0$ are listed in Table 3 and highlighted by italic.

Having compiled the thermodynamic data for all the equilibrium species, the equilibrium constants (K_1 and K_2) were determined using Eq. 8 and demonstrated in Figure 2. In subsequent calculations, it will be conventional to have simple mathematical expressions for the equilibrium constants plotted in Figure 2. Accordingly, these computational results have been subjected to regression analysis using an equation of the form

Table 2. Equilibrium Constants of Solids in NH_4Cl-$MgCl_2$-H_2O System at 298.15 K

Method	1	2	3			
ln K_1	3.0045[24]	3.0328[25]	2.8514[26]	2.86[23]	2.8625[27]	
ln K_2			10.6[28,29]	10.397[10]	10.26[30]	10.114[31]
ln K_3			9.59[29]	9.59[10]		

Table 4. Coefficients of Temperature Functions for Heat Capacities of Species

Species	$C_p = a + b\,T + c\,T^{-2}$			
	A	$10^3 b$	c	T (K) range
$Cl^-(aq)$[32,33]	−18.41	0	-2.3907×10^{-3}	
$NH_4^+(aq)$[32,33]	73.060	0	8.7864×10^{-6}	
$Mg^{2+}(aq)$[32,33]	87.085	0	-2.4652×10^{-3}	
$H_2O(l)$[34]	41.2201	70.9637	1158055.2253	273.16–400
$NH_4Cl(s)$[34]	48.3173	143.4910	−414086	273.15–400
$MgCl_2{\cdot}6H_2O(s)$[34]	241.7398	245.7940	367.4042	273.15–400

$$\ln K = k_1 + \frac{k_2}{T} + k_3 \ln T + k_4 T \tag{18}$$

with T in Kelvin. The regression coefficients are given in Table 5.

The Pitzer Ionic Interaction Parameters of Binary Systems. The accuracy of Aspen's existing Pitzer model parameters in estimating solubilities in NH_4Cl-H_2O, $MgCl_2$-H_2O, and NH_4Cl-$MgCl_2$-H_2O systems was first evaluated by comparing Aspen's prediction to experimental data. As mentioned previously, no estimation of $NH_4MgCl_3{\cdot}6H_2O$ solubility is possible with the current Aspen model. Hence, the species of $NH_4MgCl_3{\cdot}6H_2O$ with the value of equilibrium constant[10,29] at 298.15 K was added to Aspen's databank. The comparisons between the Aspen solubility prediction and the experiment in the case of binary systems are satisfactory at a wide temperature range. As it can be seen in Figure 1, however, a significant deviation of Aspen prediction from experiments is observed in the NH_4Cl-$MgCl_2$-H_2O system, and this is enlarged at elevated temperature.

Balarew et al.[10,29] have successfully represented the solubility in the NH_4Cl-$MgCl_2$-H_2O system with the Pitzer model at 298.15 K, and their results are also demonstrated in Figure 1. As it can be observed, excellent agreement with experimental is achieved by the calculation with their parameters. To explore the temperature dependence of the parameters over entire temperature range up to 373.15 K, an empirical temperature function in the form of Eq. 19 was tested for NH_4Cl-H_2O and $MgCl_2$-H_2O binary systems.[17]

$$F(T) = b_0 + b_1(T - T_r) + b_2\left(\frac{1}{T} - \frac{1}{T_r}\right) + b_3 \ln\frac{T}{T_r}, \tag{19}$$

where b_0 has a value from Balarew and Christov, F denotes $\beta^{(0)}$, $\beta^{(1)}$, and C^{ϕ}. The new ionic interaction parameters for NH_4Cl-H_2O and $MgCl_2$-H_2O systems were regressed by using the solubility data of two salts (NH_4Cl and $MgCl_2{\cdot}6H_2O$) in water at temperatures ranging from 273.15 to 388.15 K and tabulated in Table 6. With the aid of the new model parameters, the solubility of NH_4Cl and $MgCl_2{\cdot}6H_2O$ in water was calculated by using Aspen program. A comparison of experimental and predicted solubility values is presented in Figure 3. Figure 3 shows the excellent agreement between the experimental values generated by authors and the predicted solubility. The relative deviation obtained for the solubilities of the two salts at the entire temperature range is depicted in Figure 4, where the maximum deviations, 0.48% for NH_4Cl and 0.21% for $MgCl_2{\cdot}6H_2O$, are observed.

The Pitzer Mixing Parameters of NH_4Cl-$MgCl_2$-H_2O Ternary System. The SLE values of the NH_4Cl-$MgCl_2$-H_2O ternary system were predicted with the new set of binary parameters as well as the mixing parameters from Balarew and Chirstov at 298.15 K.[10,23,28,29] The agreement with the experimental values is good up to 323.15 K. When the system temperature is higher than 323.15 K, the deviations are pronounced, not even to predict at 388.15 K. Therefore, the values of $\theta_{NH_4^+,Mg^{2+}}$ and $\psi_{NH_4^+,Mg^{2+},Cl^-}$ should be further evaluated. $\theta_{NH_4^+,Mg^{2+}}$ was regressed in terms of temperature by Eq. 19 with remaining $\psi_{NH_4^+,Mg^{2+},Cl^-}$ value as Balarew and Chirstov.[10,23,28,29] It should be mentioned that the solubility data in the crystallization field of NH_4Cl were merely subjected to the regression of the mixing parameters $\theta_{NH_4^+,Mg^{2+}}$ because of the absence of equilibrium constant and thermodynamic data for $NH_4MgCl_3{\cdot}6H_2O$ as well as few solubility values for $MgCl_2{\cdot}6H_2O$ due to its narrow crystallization field. The coefficients thus obtained are listed in Table 6 with the relative deviations depicted in Figure 5, where the maximum deviation is only 4%. Furthermore, the experimental solubility data saturated with $NH_4MgCl_3{\cdot}6H_2O$ were applied to obtain the equilibrium constants of $NH_4MgCl_3{\cdot}6H_2O$. Its coefficients thus obtained are given in Table 5, and the calculated results are depicted in Figure 6. As it can be observed in the Figure, most of the deviations are less than 5% with few data points at 388.15 K exhibiting the maximum deviations (about 8%) in the $NH_4MgCl_3{\cdot}6H_2O$ crystallization field, which is probably caused by the high ionic strength.

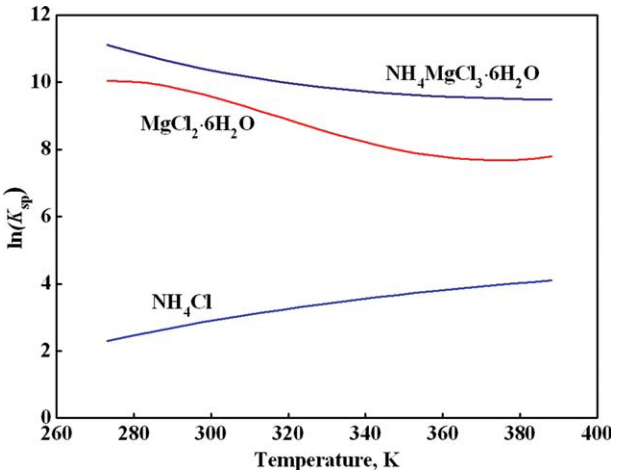

Figure 2. The logarithm of equilibrium constants for the three salts in the ternary NH_4Cl-$MgCl_2$-H_2O system.

[Color figure can be viewed in the online issue, which is available at wileyonlinelibrary.com.]

Table 5. Coefficients for Equilibrium Constants of NH_4Cl, $MgCl_2{\cdot}6H_2O$, and $NH_4Cl{\cdot}MgCl_2{\cdot}6H_2O$

Parameters	a_1	a_2	a_3	a_4	T (K) range
ln K_1	133.1239	−5693.7958	−20.8602	0.02579	273.15–400
ln K_2	167.7791	−176.3930	−31.7873	0.08161	273.15–400
ln K_3	5698.8697	−156219.64	−986.1112	1.52001	273.15–400

With the new set of parameters mentioned above, the solubilities of the NH_4Cl-$MgCl_2$-H_2O system were then calculated from 278.15 to 388.15 K. The calculated results are in good agreement with the experimental values as shown in Figure 7. A comparison of the calculated solubilities and the literature as well as the experimental data determined in this work at 278.15, 333.15, and 388.15 K is demonstrated in Figure 7, indicating that the new set of Pitzer mixing-parameter values is capable of representing the available solubility data.

Visualization of phase behavior for NH_4Cl-$MgCl_2$-H_2O ternary system

Graphical visualization of phase behavior in the form of SLE phase diagram is an indispensable tool for design and synthesis of crystallization-based separation processes.[35] To establish a feasible way to recover NH_4Cl from filtrate in the process of MgO production, the calculated and experimental phase behaviors of the ternary system are represented on an equilateral triangle in Figure 8.

In Figure 8, the solubility curves for the ternary NH_4Cl-$MgCl_2$-H_2O system at 278.15 and 388.15 K are designated as *abcd* and *ghij*, respectively. At 278.15 K, for example, *ab* represents the solubility curve of NH_4Cl (N), *bc* for $NH_4MgCl_3{\cdot}6H_2O$ (NM) and a narrow segment, *cd*, for $MgCl_2{\cdot}6H_2O$ (M). As aforementioned, the ternary NH_4Cl-$MgCl_2$-H_2O system generates the double salt, NM, resulting two kinds of double saturated point with respect to N + NM and NM + M in this system. The multiple saturation points play a very important role in fractional crystallization from solution.[36] In this work, the double saturated points for N + NM are highlighted in NH_4Cl-$MgCl_2$-H_2O ternary system because of its importance in the recovery of NH_4Cl. The calculated and experimental N + NM double saturated points are plotted in Figure 8. The relative deviations are shown in Figure 9, where a maximum deviation (about 8.6%) is exhibited at 388.15 K with other less than 5%, indicating the reasonability of the new set of parameters once again. As can be seen from the Figure 8, the double saturated curve, *bh*, with respect to N + NM intersects with the H_2O-NM line, *kl*, indicating that the concentration of $MgCl_2$ and NH_4Cl is equal in the saturated aqueous phase corresponding to the intersection, *o*. By use of this speciality, the composition and temperature with respect to the double saturated point, *o*, were calculated and determined with Aspen Plus software using the new set of parameters. The calculated temperature for the intersection, *o*, is 322 K (its calculated solubility curve designated as *eof*), below and above which the double salt, NM, behaves quite differently when water is added. Above 322 K, the addition of water causes NM to be dissolved without producing a third phase. However, below 322 K, MN can decompose with the crystallization of NH_4Cl by gradually adding water to the system. It follows that below 322 K the addition of water to NM can give rise to a system consisting of only the two phases, NH_4Cl and its saturated solution of NH_4Cl-$MgCl_2$-H_2O system. Thus, as indicated in Figure 8, for recovery of NH_4Cl from an NH_4Cl-rich mixture obtained after separation in Refs. 2 or 3, the liquid phase composition can vary as follows:

- From NH_4Cl unsaturation variety to the NH_4Cl-$NH_4MgCl_3{\cdot}6H_2O$ double saturation variety with swinging the temperature and increasing the concentration of $MgCl_2$. During this period, only NH_4Cl crystallizes.
- From the NH_4Cl-$NH_4MgCl_3{\cdot}6H_2O$ saturation variety to the $MgCl_2{\cdot}6H_2O$-$NH_4MgCl_3{\cdot}6H_2O$ double saturation variety with further increasing the concentration of $MgCl_2$. During this period, the double salt, $NH_4MgCl_3{\cdot}6H_2O$, crystallizes.
- From the double salt, $NH_4MgCl_3{\cdot}6H_2O$, variety to the NH_4Cl-$NH_4MgCl_3{\cdot}6H_2O$ double saturation variety at ex. 278.15 K with adding of water or NH_4Cl-H_2O variety.

Table 6. Temperature Coefficients of $\beta^{(0)}$, $\beta^{(1)}$, and C^{ϕ}, θ and ψ in Pitzer Model for the NH_4Cl-$MgCl_2$-H_2O System

Parameters		b_0*	b_1	b_2	b_3
NH_4Cl	$\beta^{(0)}$	0.0521	−0.010392	−457.0855	0
	$\beta^{(1)}$	0.1916	0.013809	0	0
	C^{ϕ}	−0.003	−0.0006489	−135.6252	0
$MgCl_2$	$\beta^{(0)}$	0.3511	0.0026204	0	0
	$\beta^{(1)}$	1.6512	−0.450059	0	67.7147
	C^{ϕ}	0.0065	0.00022498	0	0
Mixed	θ	−0.044	0.0071801	707.2666	0
	ψ	−0.018	0	0	0

*Refs. 10, 23, 28, and 29.

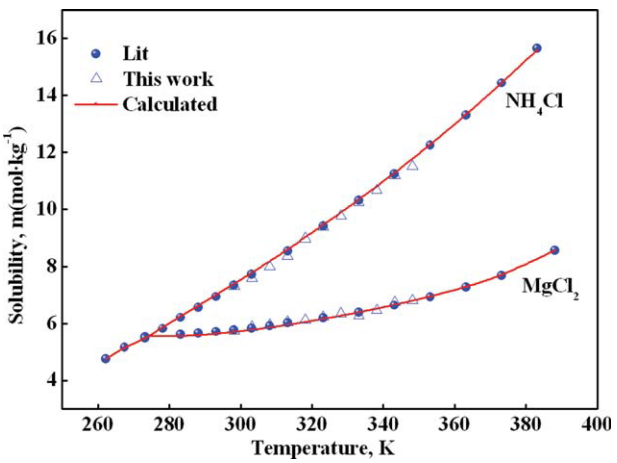

Figure 3. Solubility of NH_4Cl and $MgCl_2{\cdot}6H_2O$ in NH_4Cl-H_2O and $MgCl_2$-H_2O binary system.

[Color figure can be viewed in the online issue, which is available at wileyonlinelibrary.com.]

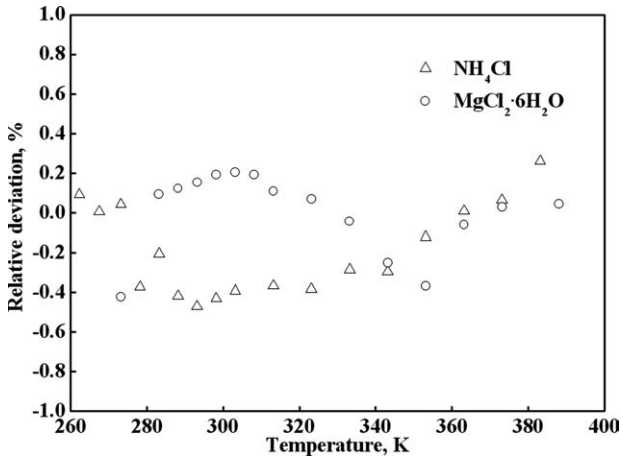

Figure 4. Relative deviation of the calculated values from Pitzer model in binary NH_4Cl-H_2O and $MgCl_2$-H_2O system.

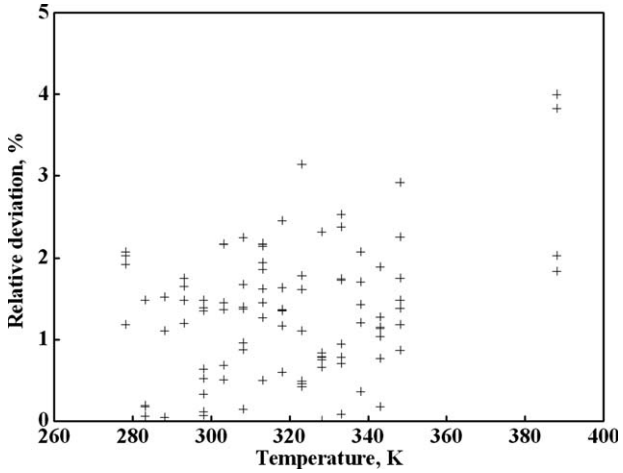

Figure 5. Relative deviation of the calculated values for NH_4Cl crystallization field from Pitzer model in ternary NH_4Cl-$MgCl_2$-H_2O system.

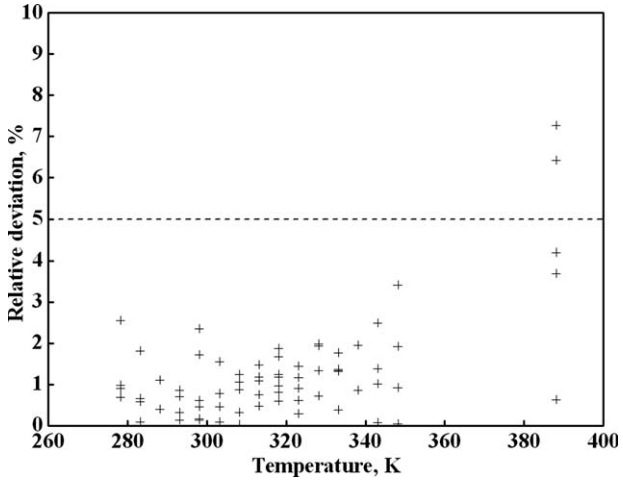

Figure 6. Relative deviation of the calculated values for $NH_4MgCl_3{\cdot}6H_2O$ crystallization field from Pitzer model in ternary NH_4Cl-$MgCl_2$-H_2O system.

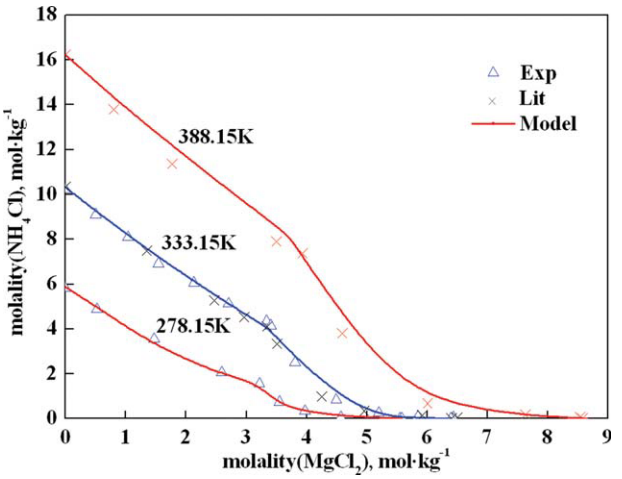

Figure 7. Solubility in the ternary NH_4Cl-$MgCl_2$-H_2O system at 278.15, 333.15, and 388.15 K.

[Color figure can be viewed in the online issue, which is available at wileyonlinelibrary.com.]

During this period, the double salt decomposes, and NH_4Cl crystallizes.

As a result of this variation, the crystalline NH_4Cl is recovered by three fractional crystallization operations, while the $MgCl_2$-rich aqueous solution with the concentration of NH_4Cl less than 0.1 mol L^{-1} is generated as the feed in the MgO production process.

Development of a new method to recover NH_4Cl in the production of MgO

With insight derived from the visualization of phase behavior for the ternary NH_4Cl-$MgCl_2$-H_2O system, a series of strategies and operations are formulated for carrying the feed NH_4Cl-H_2O mixture to the desired crystallization

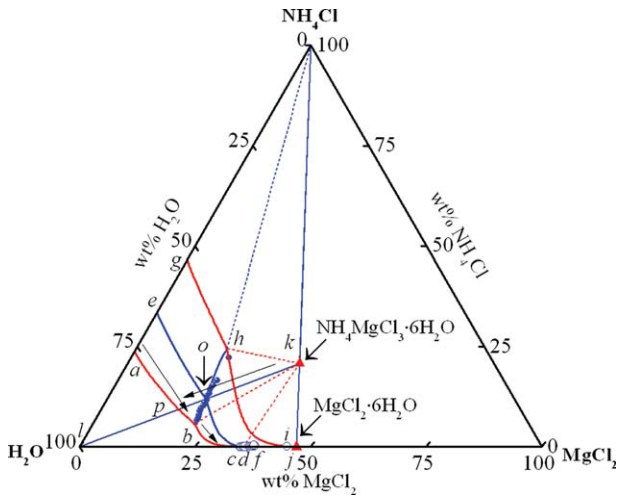

Figure 8. Phase diagram visualization and operation in recovery of NH_4Cl for the ternary NH_4Cl-$MgCl_2$-H_2O system.

[Color figure can be viewed in the online issue, which is available at wileyonlinelibrary.com.]

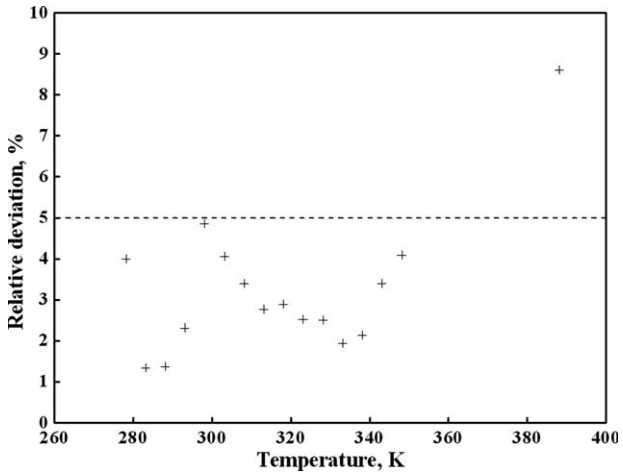

Figure 9. Relative deviation of the calculated values for multisaturated point using Pitzer model in ternary NH_4Cl-$MgCl_2$-H_2O system.

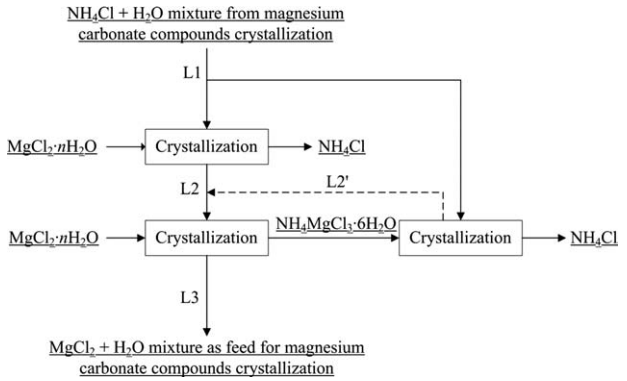

Figure 10. Principle flow sheet for the recovery of NH_4Cl in the process of MgO production.

regions, where pure solids of the targeted components can be isolated. Such operations, which include temperature swing, addition of $MgCl_2$ etc., form a preliminary crystallization-based separation scheme, and the corresponding process flow sheet for the recovery of NH_4Cl in the process of MgO production can then be generated accordingly. The new process is schematically plotted in Figure 10. In this process, NH_4Cl can be recovered by the three crystallization operations. In the first crystallization step, NH_4Cl crystallizes from an NH_4Cl-rich solution by increasing the concentration of $MgCl_2$ up to 2.5–2.7 mol L^{-1} following with a decrease of temperature. Then, in the second crystallization step, $NH_4MgCl_3{\cdot}6H_2O$ crystallizes with further increasing the concentration of $MgCl_2$ to 3.5–4 mol L^{-1} at a constant temperature. Finally, in the third crystallization step, $NH_4MgCl_3{\cdot}6H_2O$ is decomposed by addition of water (or NH_4Cl-rich solution) with the concentration of $MgCl_2$ controlled between 2.5 and 2.7 mol L^{-1} and NH_4Cl crystallizes at temperature below 322 K. After recovering NH_4Cl, an $MgCl_2$-rich solution is obtained

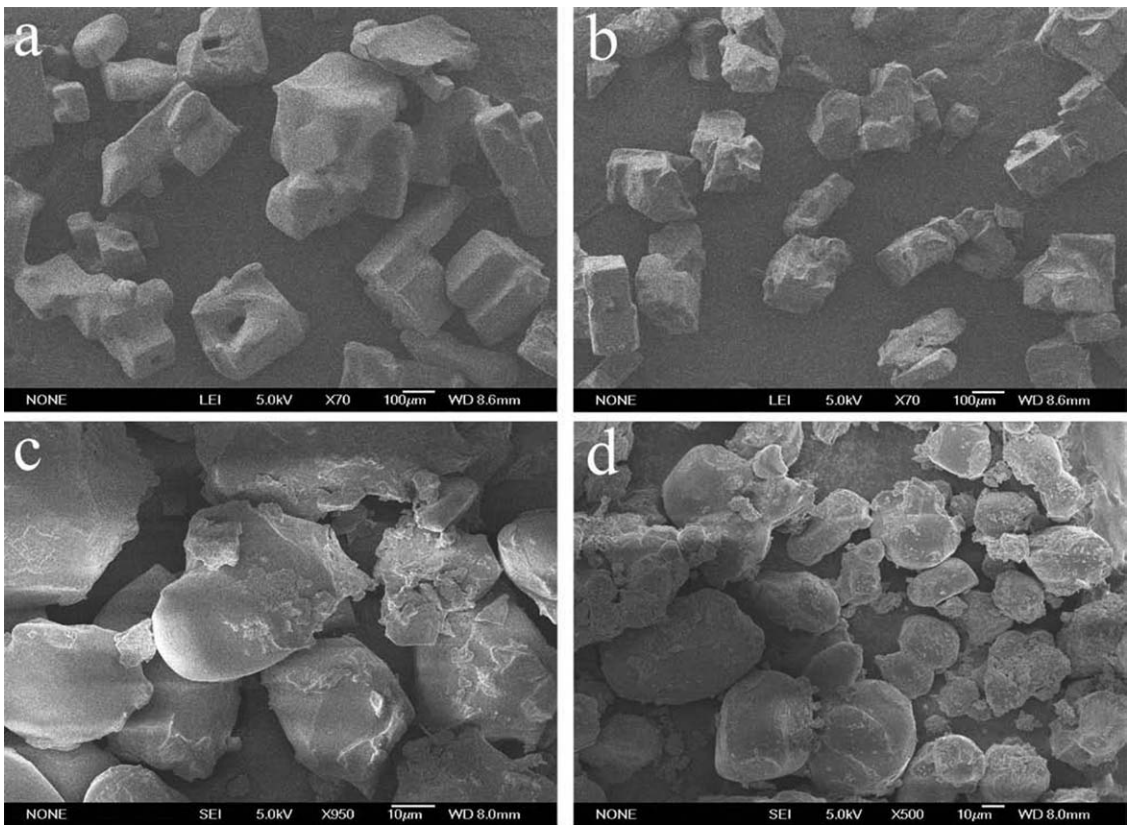

Figure 11. SEM patterns of ammonium carnallite and ammonium chloride crystal.

a, b—ammonium carnallite; c, d—ammonium chloride.

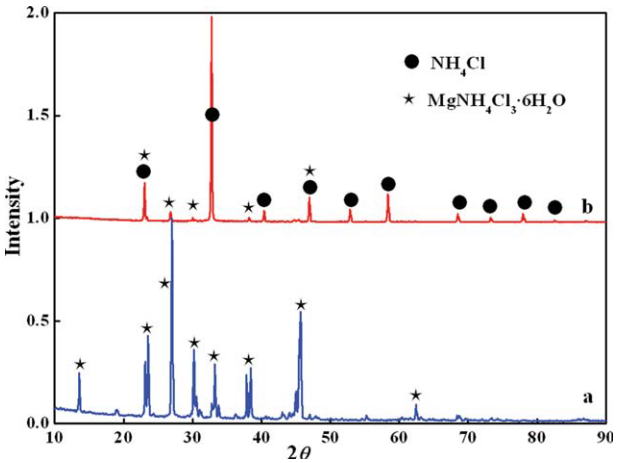

Figure 12. XRD patterns of ammonium carnallite and ammonium chloride crystal.

a—ammonium carnallite; b—ammonium chloride. [Color figure can be viewed in the online issue, which is available at wileyonlinelibrary.com.]

and served as the feed for magnesium carbonate compounds precipitation by recycling into the next matter cycle.

The recovery of NH_4Cl was successfully tested in the laboratory according to the process displayed in Figure 10. An NH_4Cl-rich solution of 4.5 mol L^{-1} at 363.15 K was used as the feed. Crystal NH_4Cl was first obtained with addition of $MgCl_2$ to 2.5 mol L^{-1} following by a decrease of temperature to 298.15 K. Then, crystal $NH_4MgCl_3{\cdot}6H_2O$ was gained with increasing the concentration of $MgCl_2$ to 3.5 mol L^{-1} at 298.15 K. Further, crystal NH_4Cl was again obtained from the decomposition of $NH_4MgCl_3{\cdot}6H_2O$ by addition of water with controlling $MgCl_2$ concentration of 2.65 mol L^{-1} at 278.15 K. The SEM image and XRD patterns of ammonium carnallite (NM) crystallized in the second step and NH_4Cl crystalline recovered from decomposition of the double salt in the third step are shown in Figures 11 and 12, respectively. It shows that the double salt crystallizes well with the size of around 100 μm, while the final product of NH_4Cl crystallizing with the size of around 30 μm.

Conclusions

A new method to recover NH_4Cl in the MgO production by three fractional crystallization operations was proposed and proved feasible in the work based on the experiment, modeling, and visualization of phase behavior for NH_4Cl-$MgCl_2$-H_2O system. The SLE values for the system of NH_4Cl-$MgCl_2$-H_2O from 278.15 to 348.15 K were determined using the isothermal dissolution method. The solubility curve at each temperature consists of three branches: broad fields of crystallization for NH_4Cl and $NH_4MgCl_3{\cdot}6H_2O$, which were used to recover NH_4Cl, along with a very narrow field of crystallization for $MgCl_2{\cdot}6H_2O$. The Pitzer model applicable to represent the solubility of the system has been successfully developed, which covers the temperature range from 278.15 to 388.15 K. The availability of the new set of temperature-dependent Pitzer parameters for concentrated NH_4Cl-$MgCl_2$-H_2O system makes it possible to meet the need of process identification and simulation in the commercial scale. The phase-equilibrium diagram generated from the model indicates that the double salt, $NH_4MgCl_3{\cdot}6H_2O$, decomposes to NH_4Cl and its saturated solution with adding of water below 322 K. This was also tested for the recovery of NH_4Cl.

Acknowledgments

The authors gratefully acknowledge the financial support of National Natural Science Foundation of China (Grant No. 2087616) and National Basic Research Program of China (973 Program, 2007CB613501, 2009CB219904).

Notation

a = parameter in heat capacity; modified Debye-Hückel parameters
b = parameter in heat capacity
B = parameter of Pitzer equation
B' = parameter of Pitzer equation
c = parameter in heat capacity
C_p = heat capacity, J mol^{-1} K^{-1}
C^{ϕ} = parameter of Pitzer equation
H^0 = standard-state enthalpy, J mol^{-1}
I = ionic strength
k = parameter in the function of solubility product
K = equilibrium constant
M = component molality, mol kg^{-1}
MX = 2-1 electrolyte, the cation is M and the anion is X
NX = 1-1 electrolyte, the cation is N and the anion is X
R = universal gas constant, J mol^{-1} K^{-1}
S^0 = standard-state entropy, J mol^{-1} K^{-1}
T = absolute temperature, K
T_r = temperature at reference state
y = ionic strength fraction of NH_4Cl

Greek letters

α = empirical parameter of Pitzer equation
$\beta^{(0)}$ = parameter of Pitzer equation
$\beta^{(1)}$ = parameter of Pitzer equation
γ = compound activity coefficient
ϕ = osmotic coefficient
θ = parameter of Pitzer equation
ψ = parameter of Pitzer equation
μ^0 = standard-state chemical potential, J mol^{-1}
ν = stoichiometric number of an ion in solutions while one mole salt dissolution
κ = stoichiometric number of an element in salt's formula (simplest)

Subscripts and superscripts

f = formation reaction
i = salt, ionic species
j = salt, ionic species
n = simple matter corresponding to element involved in salt
0 = standard state

Literature Cited

1. Mark AS. *The Chemistry and Technology of Magnesia*, 1st ed. New Jersey: Wiley, 2006.
2. Wang Y, Li ZB, Demopoulos GP. Controlled precipitation of nesquehonite by the reaction of $MgCl_2$ with $(NH_4)_2CO_3$ at 303 K. *J Cryst Growth*. 2007;310:1220–1227.
3. Cheng WT, Li ZB. Controlled supersaturation precipitation of hydromagnesite for the $MgCl_2$-Na_2CO_3 system at elevated temperatures: chemical modeling and experiment. *Ind Eng Chem Res*. 2010;49:1964–1974.
4. Huang HP, Shi Y, Li W, Chang SG. Dual alkali approaches for the capture and separation of CO2. *Energy Fuels*. 2001;15:263–268.
5. Hou TP. *Soda Engineering*. Beijing: Chemical Engineering Press, 1959.

6. Sohnel O, Garside J. *Precipitation: Basic Principles and Industrial Application*. Oxford: Butterworth Heinemann, 1995.
7. Mullin JW. *Crystallization*. Oxford: Butterworth-Heinemann, 2001.
8. Myerson AS. *Handbook of Industrial Crystallization*. Oxford: Butterworth-Heinemann, 2002.
9. William FL. *Solubilities—Inorganic and Metal-Organic Compounds*, Vol. 2, 4th ed. Washington, DC: American Chemistry Society, 1965.
10. Balarew Chr, Christov Chr, Valyashko V, Petrenko S. Thermodynamics of formation of carnallite type double salts. *J Solution Chem.* 1993;22:173–181.
11. Guendouzi ME, Azougen R. Thermodynamic properties of ternary system {yNH_4Cl + (1-y)$MgCl_2$}(aq) at 298.15 K. *Fluid Phase Equilibria*. 2007;253:81–87.
12. Guendouzi ME, Azougen R. Thermodynamic properties on quaternary aqueous solutions of chlorides charge-type 1–1*2–1*2–1: XCl + $MgCl_2$ + $CaCl_2$+H_2O with (X≡Na+; NH_{4+}). *Fluid Phase Equilibria*. 2009;287:72–79.
13. Dong M, Li ZB, Mi JG, Demopoulos GP. Solubility and stability of nesquehonite ($MgCO_3{\cdot}3H_2O$) in mixed NaCl, KCl, $MgCl_2$ and NH_4Cl solutions. *J Chem Eng Data*. 2008;53:2586–2593.
14. Dong M, Li ZB, Mi JG, Demopoulos GP. Solubility and stability of nesquehonite ($MgCO_3{\cdot}3H_2O$) in mixed NaCl + $MgCl_2$, NH_4Cl + $MgCl_2$, LiCl and LiCl + $MgCl_2$ solutions. *J Chem Eng Data*. 2009;54:3002–3007.
15. Ji XY, Lu XH, Zhang LZ, Bao NZ, Wang YR, Shi J, Lu Benjamin CY. A further study of solid-liquid equilibrium for the NaCl-NH_4Cl-H_2O system. *Chem Eng Sci*. 2000;55:4993–5001.
16. Pitzer KS. Thermodynamics of electrolytes. I. Theoretical basis and general equations. *J Phys Chem.* 1973;77:268–277.
17. Pitzer KS. *Activity Coefficients in Electrolyte Solutions*, 2nd ed. Boca Raton: CRC Press, 1991.
18. Haynes HW Jr. Thermodynamic solution model for trona brines. *AIChE J*. 2003;49:1883–1894.
19. Liu HX, Papangelakis VG. Chemical modeling of high temperature aqueous processes. *Hydrometallurgy*. 2005;79:48–61.
20. Haghtalab A, Papangelakis VG, Zhu XT. The electrolyte NRTL model and speciation approach as applied to multicomponent aqueous solutions of H_2SO_4, $Fe_2(SO_4)_3$, $MgSO_4$ and $Al_2(SO_4)_3$ at 230–270°C. *Fluid Phase Equilibria*. 2004;220:199–209.
21. Liu HX, Papangelakis VG. Thermodynamic equilibrium of the O_2-$ZnSO_4$-H_2SO_4-H_2O system from 25 to 250°C. *Fluid Phase Equilibria*. 2005;234:122–130.
22. Barrow GM. *Physical Chemistry*, 6th ed. New York: McGraw-Hill, 1996.
23. Christov Chr, Petrenko S, Balarew Chr, Valyashko VI. Calculation of the Gibbs energy of mixing in crystals using Pitzer's model. *J Solution Chem.* 1994;23:795–812.
24. Lu X, Zhang L, Wang Y, Shi J. Prediction of activity coefficients of electrolytes in aqueous solutions at high temperatures. *Ind Eng Chem Res.* 1996;35:1777–1784.
25. Barin I, Knacke O. *Thermochemical Properties of Inorganic Substances*, 1st ed. Berlin: Springer, 1973.
26. Staveley LAK, Davies NJ. The thermodynamics of mixed crystals of (ammonium chloride + ammonium bromide) IV. The excess Gibbs free energy, excess enthalpy, and excess entropy at the temperature T = 298.15 K and at T = 0. *J Chem Thermodyn.* 1995;27:787–799.
27. Harmer WJ, Wu YC. Osmotic coefficients and mean activity coefficients of uni-univalent electrolytes in water at 25°C. *J Phys Chem Ref Data.* 1972;1:1047–1100.
28. Christov Chr, Balarew Chr, Petrenko S, Valyashko VI. Investigation of the aqueous lithium and magnesium halide systems. *J Solution Chem.* 1994;23:595–604.
29. Christov Chr. Thermodynamics of formation of double salts and mixed crystals from aqueous solutions. *J Chem Thermodyn.* 2005;37:1036–1106.
30. Harvie C, Moller N, Weare J. The prediction of mineral solubilities in natural waters: the Na-K-Mg-Ca-H-Cl-SO_4-OH-HCO_3-CO_3-CO_2-H_2O system from zero to high concentration at 25°C. *Geochim Cosmochim Acta*. 1984;48:723–751.
31. Christov Chr. Isopiestic determination of the osmotic coefficients of an aqueous $MgCl_2$ + $CaCl_2$ mixed solution at (25 and 50)°C. Chemical equilibrium model of solution behavior and solubility in the $MgCl_2$ + H_2O and $MgCl_2$ + $CaCl_2$ + H_2O systems to high concentration at (25 and 50)°C. *J Chem Eng Data*. 2009;54:627–635.
32. Shock EL, Helgeson HC. Calculation of the thermodynamic and transport properties of aqueous species at high pressures and temperatures: correlation algorithms for ionic species and equation of state predictions to 5 Kb and 1000°C. *Geochim Cosmochim Acta.* 1988;52:2009–2036.
33. Shock EL, Sassani DC, Willis M, Sverjensky DA. Inorganic species in geologic fluids: correlations among standard molal thermodynamic properties of aqueous ions and hydroxide complexes. *Geochim Cosmochim Acta*. 1997;61:907–950.
34. OLI Systems, Inc. Available at: http://www.olisystem.com/. Accessed October 20, 2009.
35. Kwok KS, Ng KM, Taboada ME, Cisternas LA. Thermodynamics of salt lake system: representation, experiments, and visualization. *AIChE J*. 2008;54:706–727.
36. Cisternas LA, Rudd DF. Process design for fractional crystallization from solution. *Ind Eng Chem Res*. 1993;32:1993–2005.

Manuscript received Mar. 1, 2010, revision received Apr. 29, 2010, and final revision received Jun. 25, 2010.